JOURNAL OF VIROLOGY, Feb. 2008, p. 1946–1958 Vol. 82, No. 4
0022-538X/08/$08.00+0 doi:10.1128/JVI.02136-07

Epstein-Barr Virus Latent Membrane Protein 1 Induces Cellular MicroRNA miR-146a, a Modulator of Lymphocyte Signaling Pathways▽†

Jennifer E. Cameron,[1,2] Qinyan Yin,[1,2,3] Claire Fewell,[3] Michelle Lacey,[4] Jane McBride,[3] Xia Wang,[3] Zhen Lin,[3] Brian C. Schaefer,[5] and Erik K. Flemington[1,2,3]*

Louisiana Cancer Research Consortium,[1] Tulane Cancer Center,[2] Department of Pathology,[3] and Department of Mathematics,[4] Tulane University, New Orleans, Louisiana, and Department of Microbiology and Immunology, Uniformed Services University of the Health Sciences Center, Bethesda, Maryland[5]

Received 27 September 2007/Accepted 20 November 2007

The Epstein-Barr virus (EBV)-encoded latent membrane protein 1 (LMP1) is a functional homologue of the tumor necrosis factor receptor family and contributes substantially to the oncogenic potential of EBV through activation of nuclear factor κB (NF-κB). MicroRNAs (miRNAs) are a class of small RNA molecules that are involved in the regulation of cellular processes such as growth, development, and apoptosis and have recently been linked to cancer phenotypes. Through miRNA microarray analysis, we demonstrate that LMP1 dysregulates the expression of several cellular miRNAs, including the most highly regulated of these, miR-146a. Quantitative reverse transcription-PCR analysis confirmed induced expression of miR-146a by LMP1. Analysis of miR-146a expression in EBV latency type III and type I cell lines revealed substantial expression of miR-146a in type III (which express LMP1) but not in type I cell lines. Reporter studies demonstrated that LMP1 induces miR-146a predominantly through two NF-κB binding sites in the miR-146a promoter and identified a role for an Oct-1 site in conferring basal and induced expression. Array analysis of cellular mRNAs expressed in Akata cells transduced with an miR-146a-expressing retrovirus identified genes that are directly or indirectly regulated by miR-146a, including a group of interferon-responsive genes that are inhibited by miR-146a. Since miR-146a is known to be induced by agents that activate the interferon response pathway (including LMP1), these results suggest that miR-146a functions in a negative feedback loop to modulate the intensity and/or duration of the interferon response.

The Epstein-Barr virus (EBV) infects over 90% of the human population worldwide. Like other members of the gammaherpesvirus family, EBV typically establishes a lifelong, predominantly asymptomatic infection in its host (20). Nevertheless, persistent EBV infection can result in a number of malignancies, including Burkitt's lymphoma, Hodgkin's lymphoma, nasopharyngeal carcinoma, and lymphoproliferative diseases in immunosuppressed individuals (34). EBV oncogenesis is principally associated with latency, during which only a limited subset of the full repertoire of viral genes is transcribed. Latency gene expression is classified into three groups. In cells exhibiting latency type I, the EBV nuclear protein EBNA1 is the only viral protein-coding gene that is expressed. Latency type II is characterized by expression of EBNA1 as well as latent membrane proteins (LMPs) 1, 2A, and 2B. Type III latency cells express the entire repertoire of latency-associated EBV gene products. Six of these encode nuclear proteins (EBNA1, EBNA2, EBNA3A, EBNA3B, EBNA3C, and EBNA-LP), and three encode membrane proteins (LMP1, LMP2A, and LMP2B) (20). In addition to these protein-coding genes, the noncoding RNAs EBER1 and EBER2 and a set of EBV encoded microRNAs (miRNAs) are expressed in all three forms of latency (34).

Of the viral latency genes expressed in EBV-associated malignancies, LMP1 is the most highly implicated in tumor formation (for a review, see reference 42). First, although different EBV-associated tumors exhibit distinct latency gene expression patterns, LMP1 is expressed in all but Burkitt's lymphoma. Second, LMP1 is required for EBV-mediated transformation of lymphocytes in vitro, and it has the ability to transform rodent fibroblasts. Finally, transgenic mice expressing LMP1 from an immunoglobulin promoter develop B-lymphocyte tumors more frequently than nontransgenic mice (22).

LMP1 is a six-transmembrane, constitutively active signaling molecule that functionally mimics cellular tumor necrosis factor receptor (TNFR) family members. While the transmembrane domain is required for aggregation and constitutive activation of LMP1 (11, 12, 24), two cytoplasmic domains, referred to as C-terminal activator regions 1 and 2 (CTAR-1 and CTAR-2), have been shown to be critical for the transforming properties of LMP1 (17–19). Together, these signaling domains act through cellular TNFR-associated factors (TRAFs) and other cell signaling molecules to activate transcription factors, including nuclear factor κB (NF-κB), activator transcription factor 2 (via p38 mitogen-activated protein kinase), and AP-1 (via c-Jun N-terminal kinase) (3, 6, 8–10, 16–18, 29). Through the hijacking of these cell signaling pathways, LMP1 is able to manipulate host cellular processes that regulate cell proliferation, migration, and apoptosis and thereby contribute to cellular immortalization and tumorigenesis.

* Corresponding author. Mailing address: Tulane University Health Sciences Center, 1430 Tulane Ave., SL79, New Orleans, LA 70112. Phone: (504) 988-1167. Fax: (504) 988-5516. E-mail: eflemin@tulane.edu.

† Supplemental material for this article may be found at http://jvi.asm.org/.

▽ Published ahead of print on 5 December 2007.

Among the pathways regulated by LMP1 is the interferon (IFN) type I (alpha/beta) pathway, which is induced in part through the induction of IFN regulatory factor 7 (IRF7) (15, 31).

Recently, a novel class of small (~22-nucleotide) RNA molecules referred to as miRNAs have been identified as important regulators of a broad array of cell processes in mammals, including proliferation, differentiation, and apoptosis. MicroRNAs function predominantly through the inhibition of mRNA translation via imperfect complementary sequence recognition in the 3′ untranslated region (UTR) of target mRNA transcripts. The binding of microRNA/protein complexes to the 3′ untranslated regions (and less frequently the 5′ untranslated or coding sequence) causes transport to a perinuclear compartment referred to as GW or P bodies, thereby sequestering the mRNA away from the Golgi apparatus (25–27). In this compartment it is thought that at least some of these mRNAs can then be subjected to degradation (25, 26).

MicroRNAs have been implicated in regulation of immune responses. The BIC transcript, which is upregulated in B-cell lymphomas, including EBV-associated lymphoproliferative diseases, encodes miR-155. Knockout mice deficient in BIC/miR-155 were unable to generate a protective immune response in a *Salmonella* postimmunization challenge model and were impaired in antibody production, class switching, and production of interleukin-2 (IL-2) and IFN-γ when immunized with tetanus toxin fragment C (35). Interestingly, miR-155 transgenic mice developed B-cell lymphomas (5), suggesting that some miRNAs that are critical to normal cell functions may have oncogenic potential when inappropriately expressed.

Regulation of innate immune responses by miRNAs has also been demonstrated. Toll-like receptor (TLR) signaling in monocytes induced miR-155 as well as miR-132 and miR-146a expression (37). Further exploration of the response of miR-146a in innate immune pathways demonstrated that miR-146a is induced by multiple TLRs recognizing bacterial stimuli, including lipopolysaccharide, but not those that recognize viral stimuli (37). Interestingly, Taganov et al. identified TRAF6 and IL-1 receptor-associated kinase 1 (IRAK1) as two potential targets of miR-146a using 3′ UTR reporter analysis (37). Since these two factors are key mediators of TLR and IL-1 signaling pathways, they suggested the possibility that miR-146a can inhibit endogenous TRAF6 and IRAK1 expression and thereby feedback to inhibit TLR and IL-1 signaling (1, 37).

LMP1 has been shown to regulate a large number of mRNA transcripts that likely play roles in the life cycle of the virus (4). Since LMP1 predominantly influences the cell through activation of transcription, we assessed whether LMP1 alters the expression of miRNAs that play a role in LMP1-regulated pathways. Through microarray analysis, we identified cellular miRNA species that are regulated by LMP1. While this analysis revealed the LMP1-mediated induction of miR-146a, changes in other miRNAs shown previously to be induced by TLR signaling were not observed, suggesting distinctions between these signaling pathways leading to microRNA signaling. We also provide evidence that miR-146a negatively modulates the interferon response pathway, which may be a component of a negative feedback loop.

MATERIALS AND METHODS

Maintenance of cell lines. Lymphocyte cell lines (IB4, X50-7, Rael, Akata, JY, JC5, P3HR1, Mutu, and BL30) were maintained in RPMI medium plus 10% fetal calf serum and 0.5% penicillin-streptomycin. Epithelial cell lines (HEK293 and A549) were maintained in Dulbecco's modified Eagle's medium (DMEM) plus 10% fetal calf serum and 0.5% penicillin-streptomycin. Retrovirally transduced EBNA-1 dominant negative (EBV-negative) Mutu clone 3 cells were maintained in RPMI medium plus 10% fetal calf serum, 0.5% penicillin-streptomycin, 1 μg/ml puromycin, and 1 mg/ml gentamicin. The same selective medium that was used for the EBV-negative Mutu clone 3 cells was used for Mutu clone 3 cells transduced with pEHyg or pEHyg-FLAG-LMP1 retroviruses, with the addition of 250 μg/ml hygromycin.

Plasmid cloning. To generate dominant negative forms of EBNA1, full-length EBNA1 was first excised from the plasmid pCEP4 with ClaI and SacII. Since the SacII digestion cleaves the last few carboxy-terminal amino acids from the EBNA1 reading frame, two adaptors were synthesized which together encode the terminal amino acids from EBNA1 plus a BglII overhang (Adaptor 1-sense, 5′-GGAGGGTGATGACGGAGATGACGGAGATGAA-3′; Adaptor 1-antisense, 5′-CATCACCTCCTTCATCTCCGTCATCTCCGTCATCACCCTCCG C-3′; Adaptor 2-sense, 5′-GGAGGTGATGGAGATGAGGGTGAGGAAGG GCAGGAGTGA-3′; Adaptor 2-antisense, 5′-GATCTCACTCCTGCCCTTCC TCACCCTCATCTC-3′). The ClaI/SacII EBNA1 fragment was ligated to an EcoRI- and BglII-cut pMSCV-neo vector in the presence of Adaptor 1 plus Adaptor 2 and an EcoRI/ClaI adaptor. Ligations were carried out in the presence of 1 μl T4 polynucleotide kinase to phosphorylate adaptors during the ligation reaction. This construction led to the generation of pMSCV-neo-EBNA1wt. Next, pMSCV-neo-E1dn was generated from this plasmid by digesting pMSCV-neo-EBNA1wt with EcoRI and ApaI to excise the amino-terminal EBNA1 sequences. The resulting vector plus carboxyl-terminal EBNA1 sequences were then ligated to three adaptors which, when linked together, contain a translation initiation sequence, an hemagglutinin epitope tag, and the simian virus 40 nuclear localization signal, plus an EcoRI overhang at the 5′ end and an ApaI overhang at the 3′ end (DN adaptor 1-sense, 5′-AATTCTGCTGAAGAT GATGGCCTATCCTTATG-3′; DN adaptor 1-antisense, 5′-CATCATCTTCA GCAG-3′; DN adaptor 2-sense, 5′-ATGTGCCTGACTATGCCGCCCCAAAG AAA-3′; DN adaptor 2-antisense, 5′-CATAGTCAGGCACATCATAAGGAT AGGC-3′; DN adaptor 3-sense, 5′-AAGCGAAAGGTGGCCGGCC-3′; DN adaptor 3-antisense, 5′-GGCCACCTTTCGCTTTTTCTTTGGGGCGG-3′). Ligations were carried out in a standard ligation reaction mixture except that 1 μl of T4 polynucleotide kinase was added to phosphorylate adaptors during the ligation reaction. This strategy generated pMSCV-neo-EBNA1dn. The pMSCV-puro-EBNA1dn construct was derived from this plasmid by simply excising the hemagglutinin/nls/EBNA1dn cassette from pMSCV-neo-EBNA1dn and transferring it to pMSCV-puro using appropriate standard cloning adaptors. All constructs were verified by sequence analysis.

The pEhyg-FLAG-LMP1 vector was generated by excising FLAG-LMP1 sequences from pcDNA3-FLAG-LMP1 (generous gift of Nancy Raab-Traub) with HindIII and NotI and cloning into XhoI- and NotI-digested pEhyg using a HindIII/XhoI adaptor (5′-TCGAGGCTGCAGGCA-3′ and 5′-AGCTTGCCTG CAGCC-3′). Cloning was analyzed by diagnostic digest, and the LMP1 insert was sequenced in its entirety.

The pEhyg-miR-146a vector was generated by amplifying a 452-bp sequence containing the miR-146a hairpin (nucleotides 4721752 to 4722203 of chromosome 5; NCBI reference assembly) from Mutu cell genomic DNA by PCR and cloned downstream from the hygromycin resistance gene of the vector pEhyg (36).

The miR-146a promoter/luciferase reporter construct was made by amplifying the human miR-146a promoter extending from −1153 to +21 relative to the start site from Mutu genomic DNA by PCR using the primers 5′-GCAGCTAG CTTT CGGTCCATGAGCACGT-3′ (forward primer) and 5′-GCAAAGCTTA GCGGTCAAGCGTCTTGG-3′ (reverse primer). The isolated fragment was digested with NheI and HindIII and cloned into NheI- and HindIII-cut pGL3basic (Promega). The entire promoter region was then sequenced, and no discrepancies were identified relative to the GenBank genomic sequence.

Mutagenesis of the miR-146a reporter plasmid was carried out using a QuikChange II site-directed mutagenesis kit (Stratagene) and the following oligos: 5′-CG GAG AGT ACA GAC CTC GAG CCT GGG GAC CCA G-3′ and 5′-CTG GGT CCC CAG GCT CGA GGT CTG TAC TCT CCG C-3′ (c-Ets); 5′-CAG GCT GCT CCT GAC CTC GAG TGC AAG AGG GTC CCC-3′ and 5′-GGG GAC CCT CTT GCA CTC GAG GTC AGG AGC AGC CTG-3′ (c-Myc); 5′-CAC TGC CAG GCT GGC TCG AGC CAT TCC GGC CCA G-3′ and 5′-CTG GGC CGG AAT GGC TCG AGC CAG CCT GGC

AGT G-3′ (HSF2); 5′-CGA TAA AGC TCT CGG CTC GAG CCC GCG GGG CTG CGG-3′ and 5′-CCG CAG CCC CGC GGG CTC GAG CCG AGA GCT TTA TCG-3′ (distal NF-κB); 5′-GAG GGA TCT AGA AGG CTC GAG CCA GAG AGG GTT AGC-3′ and 5′-GCT AAC CCT CTC TGG CTC GAG CCT TCT AGA TCC CTC-3′ (proximal NF-κB), 5′-GAA ATG GAA TAA AAG CCT CGA GAA ATA GGC CTT AGC TG-3′ and 5′-CAG CTA AGG CCT ATT TCT CGA GGC TTT TAT TCC ATT TC-3′ (Oct-1); 5′-CCG GCC CAG CCT CCT CGA GCC TCG CTG TGC C-3′ and 5′-GGC ACA GCG AGG CTC GAG GAG GCT GGG CCG G-3′ (PU.1). In each case, the core transcription factor binding site was replaced with a XhoI restriction site. Mutations were initially screened by digesting with XhoI and then verified by sequence analysis.

Transfection and luciferase expression analysis. Mutant and wild-type miR-146a promoter-reporter vectors were cotransfected with pSG5 (control) or pSG5-LMP1 expression constructs into Mutu EBNA-1 dominant negative clone 3 cells using Lipofectamine reagent (Invitrogen) according to the manufacturer's instructions. Cells were harvested 48 h posttransfection and analyzed for luciferase reporter activity using Promega firefly luciferase assay reagents according to the manufacturer's protocol.

BLAST analysis of miR-146a promoter versus mouse genome. Two kilobases of sequence upstream and 190 bp downstream from the miR-146a start site in humans (reported by Taganov and Baltimore [37]) was used to analyze with BLAST the mouse genome, using the NCBI blastN algorithm with default settings. The two homologies shown in Fig. 5, below, were identified as the only hits, and they correspond to nucleotides 8703897 to 8703794 and 8703618 to 8703488 of mouse chromosome 11 (NCBI reference assembly).

Retroviral infections. Transient-transfection experiments were performed by using a modified version of the calcium phosphate precipitation procedure (a detailed protocol is available at http://www.flemingtonlab.com). Briefly, 10^6 HEK293 cells were plated onto 100-mm-diameter tissue culture dishes. The following day, the medium was replaced with 8 ml of fresh supplemented DMEM; 4 h later, DNA precipitates were generated by mixing 0.5 ml of 1× HEPES-buffered saline (0.5% HEPES, 0.8% NaCl, 0.1% dextrose, 0.01% anhydrous Na_2HPO_4, 0.37% KCl [pH 7.10]) with a total of 30 μg of plasmid DNA (10 μg retroviral vector plus 10 μg G protein of vesicular stomatitis virus expression vector, plus 10 μg pVPACK dGI packaging vector). A total of 30 μl of 2.5 M $CaCl_2$ was added, and samples were mixed immediately. Precipitates were allowed to form at room temperature for 20 min before being added dropwise to cells. Cells were incubated at 37°C with 5% CO_2 for 16 h before the medium was replaced with 10 ml of fresh DMEM (plus 10% fetal bovine serum).

Forty-eight hours later, viral supernatants were collected and subjected to one round of centrifugation followed by filtration through a 0.45-μm surfactant-free cellulose acetate membrane filter. Infections were carried out in six-well plates with 1 ml virus plus 10^6 appropriate B cells suspended in 1 ml DME plus 10% fetal bovine serum. Polybrene was added to a final concentration of 12 mg/ml, and the mixture was mixed by gently rocking. Cells were spun in six-well plates at 1,000 × *g* for 1 h followed by a 4-h incubation at 37°C, 5% CO_2. Cells were then collected, spun down, and resuspended in 2 ml RPMI (plus 10% fetal bovine serum, penicillin, streptomycin, and glutamine) per well. Cells were cultured for 2 days prior to antibiotic selection.

Generation of EBV-negative Mutu clones. Mutu I cells were serially infected with either a control retrovirus (pMSCV-neo followed by pMSCV-puro) or a retrovirus containing the dominant negative EBNA1 (pMSCV-neo-E1dn followed by pMSCV-puro-E1dn). Infection with the pMSCV-puro-based virus was done 3 days after pMSCV-neo-based infections. Cells were selected for 7 days, after which cells were cloned by limiting dilution. EBV-negative clones were identified by PCR analysis of genomic DNA for the presence of DNA from the BamHI Z, BamHI R, and BamHI Q fragments. Further verification that clones were EBV negative was carried out by reverse transcription-PCR (RT-PCR) analysis of EBNA1 transcripts, Cp-initiated transcripts, Wp transcripts, and LMP1 and LMP2 transcripts both before and after treatment with 5-azacytidine. By all accounts, Mutu E1dn Cl.3 cells were found to be EBV negative.

RNA isolation. RNAs used for miRNA array analysis and for assessing mature miRNAs were generated by a modified TRIzol method. Cells were stained with trypan blue and counted, and 10^7 cells were pelleted by centrifugation. Cells were suspended in TRIzol reagent (Invitrogen) and processed as per the manufacturer's protocol up through the addition of isopropanol. Samples were allowed to precipitate in isopropanol overnight at −20°C. Samples were then centrifuged at 12,000 × *g* for 30 min at 4°C. Isopropanol was decanted, and nucleic acid pellets were resuspended in 200 μl nuclease-free water. RNA was then precipitated again by adding 20 μl 3 M NaO-acetate and 0.5 ml of 100% ethanol and incubating overnight at −20°C. Samples were centrifuged at 12,000 × *g* for 30 min at 4°C, ethanol was decanted, and samples were washed once with 75% ethanol and allowed to air dry for no more than 10 min. RNA pellets were resuspended in nuclease-free water, quantitated by UV spectrophotometry, aliquoted, and stored at −80°C.

RNAs used for mRNA arrays and for assessing the levels of primary miR-146a were generated using a Qiagen RNeasy kit. Total RNA was isolated from 10^7 cells using the RNeasy kit according to the manufacturer's protocol. The RNA was eluted from the column using 50 μl nuclease-free water, quantitated, and stored at −80°C.

Real-time qRT-PCR for mature miRNA and primary transcript (pri-miRNA). To quantitate mature miRNA expression, total RNA isolated by a modified TRIzol protocol (see "RNA isolation," above) was polyadenylated and reverse transcribed using the NCode miRNA first-strand synthesis kit (Invitrogen) according to the manufacturer's instructions. The resulting cDNA was subjected to real-time quantitative RT-PCR (qRT-PCR) using the NCode universal reverse primer (Invitrogen) in conjunction with a sequence-specific forward primer for miR-146a (forward primers for NCode miRNA detection are the exact sequence of the mature miRNA). Similarly, U6 small nuclear RNA was quantified using the NCode universal reverse primer and a U6-specific primer (5′-CTCGCTTC GGCAGCACA-3′). A master mix was prepared for each PCR run, which included Sybr green Supermix plus UDG (Invitrogen), fluorescein-NIST traceable dye, and 100 nM forward and reverse primers. Amplification consisted of 2 min at 50°C and 2 min at 95°C, followed by 40 cycles of 95°C for 15 s and 60°C for 30 s.

Total RNA prepared by Qiagen RNeasy column extraction was DNase treated and reverse transcribed using random hexamer primers and SuperScript III reverse transcription enzyme mix and reagents (Invitrogen) according to the manufacturer's instructions. Primary transcript miR-146a expression was quantified using specific forward (5′-TGAGAACTGAATTCCATGGGTT-3′) and reverse (5′-ATCTACTCTCTCCAGGTCCTCA-3′) primers at a 200 nM concentration in a reaction mixture consisting of Sybr green Supermix plus UDG and fluorescein-NIST traceable dye. Cycling parameters were as follows: 2 min at 50°C and 2 min at 95°C, followed by 40 cycles of 95°C for 30 s and 60°C for 30 s. Glyceraldehyde 3-phosphate dehydrogenase (GAPDH) was quantified similarly; the primer sequences have been published elsewhere (40).

Melt curve analysis was performed at the end of every qPCR run. Samples were tested in triplicate. Real-time PCR was performed on Bio-Rad iCyclers (MyIQ, IQ4, or IQ5), and data analysis was performed using Bio-Rad IQ5 v2 software. Measures taken to prevent and identify PCR contamination included maintaining a physically separate, nucleic acid-free area with designated equipment for PCR setup and using both no-template controls and no-reverse transcription controls in every experiment. A standard dilution curve, generated by serially diluting a pooled stock of positive control cDNAs, was included in each run. Experiments were repeated if controls did not behave as predicted.

Relative expression was calculated for each test sample by the standard curve method (for formulas, see the ABI Prism 7700 Sequence Detection System User Bulletin 2: Relative Quantitation of Gene Expression; Applied Biosystems, Foster City, CA). Relative quantities of each test sample were extrapolated from the standard curve run concurrently with the sample, and the values were normalized to U6 small nuclear RNA (mature miRNA NCode assays) or GAPDH (primary transcript assays). The normalized values were then compared to a calibrator sample within the run. Data are presented as the expression level relative to the calibrator, with the standard error of the mean of triplicate measures for each test sample.

Cellular miRNA microarray analysis. Small RNA isolation and hybridization were performed by LC Sciences (Houston, TX). Briefly, small RNA species were isolated from total RNA by column exclusion. The concentrated small RNAs were 3′-polyadenylated with poly(A) polymerase. A nucleotide tag was then ligated to the poly(A) tails. The tagged RNAs were hybridized to a μParaflo superfluidic array chip containing probes for human and viral microRNA sequences and were subsequently labeled in a second hybridization reaction with Cy3 and Cy5 dendrimer dyes. After overnight hybridization, arrays were stringently washed and scanned on an Axon GenePix 4000B laser scanner (Axon Instruments). Data extraction and imaging were performed using ArrayPro software (Media Cybernetics).

Each array compared RNA isolated from control (Mutu plus pEHyg) and experimental (Mutu plus pEHyg-FLAG-LMP1) cells. Five separate arrays were performed, utilizing five independent pairs of RNA preparations. The most up-to-date chip available for analysis was used (containing probes for all human miRNA listed in the Sanger Institute miRBase, release 9.1, totaling 470 unique miRNAs). Additional probes (108 unique sequences) for viral miRNA expression were included on each chip. Each probe was repeated in sextuplicate. Dye swap experiments were executed to control for labeling bias. Data within each individual chip were adjusted by subtraction of background fluorescence (calculated as the median of the lower 5 to 25% of signal intensities) followed by normalization of the data to the statistical median of all detectable signals.

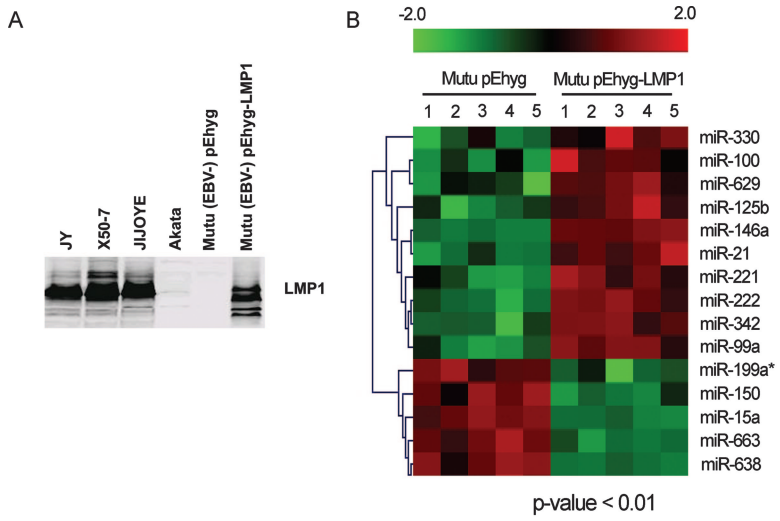

C

		Mutu pEhyg	Mutu pEhyg-LMP1	Log2 (LMP1/Cntl)
MicroRNA Reporter	p-value	Mean	Mean	
hsa-miR-146a	1.26E-07	61	1,000	4.03
hsa-miR-15a	6.46E-06	18,938	13,074	-0.53
hsa-miR-663	2.77E-05	1,633	421	-1.95
hsa-miR-222	3.93E-05	349	744	1.09
hsa-miR-21	1.83E-04	17,253	33,126	0.94
hsa-miR-99a	1.85E-04	734	1,532	1.06
hsa-miR-342	3.93E-04	168	556	1.73
hsa-miR-150	4.21E-04	697	369	-0.92
hsa-miR-638	7.49E-04	9,255	3,803	-1.28
hsa-miR-221	9.09E-04	369	726	0.98
hsa-miR-125b	1.35E-03	2,176	3,792	0.80
hsa-miR-199a*	1.83E-03	538	251	-1.10
hsa-miR-100	3.52E-03	111	326	1.56
hsa-miR-330	7.49E-03	130	230	0.82
hsa-miR-629	8.56E-03	134	193	0.53

FIG. 1. EBV LMP1 alters expression profiles of cellular miRNA. Microarray analysis of miRNA expression was performed on RNA isolated from control (Mutu pEHyg) and LMP1-expressing (Mutu pEHyg-LMP1) EBV-negative Mutu Cl.3 cells. Five separate RNA pairs were hybridized to miRNA arrays, and the data were combined for analysis. A. Western blot analysis of LMP1 expression in the EBV-positive latency type III cell lines JY, X50-7, and Jijoye, the type I latency cell line Akata, and in control or LMP1-transduced EBV-negative Mutu cells. B. Cluster analysis of miRNAs significantly altered by LMP1 at a P level of <0.01. C. MicroRNAs significantly ($P < 0.01$) regulated by LMP1, showing mean signal intensities and log-transformed ratios.

Variation among arrays introduced by differences in experimental conditions (i.e., sample preparation, dye labeling, chip quality, and scanning variations) was corrected by normalization of the data by the cyclic LOWESS (locally weighted regression) method (2). Intensity values were then $\log_2$ transformed and further normalized and centered using the following equation: [($\log_2$ intensity value) − [(mean of values across all samples for the individual gene)/(standard deviation of values across all samples for the individual gene)]. The ratio of expression between control and test samples was normalized for clustering analysis by the following equation: [$\log_2$(ratio)]/[(standard deviation of $\log_2$(ratio)]. Statistical comparison of control (Mutu-pEHyg) and test (Mutu-pEHyg-FLAG-LMP1) sample miRNA expression levels was performed using t tests, and corresponding P values were calculated (32). MicroRNAs showing differential expression at the P levels of <0.10, <0.05, and <0.01 were selected for clustering analysis, which was performed using a hierarchical method based on average linkage and a Euclidean distance metric (7). All data calculations were performed by LC Sciences. Clustering plots were created using TIGR MeV (multiple experimental viewer) software (The Institute for Genomic Research).

Cellular mRNA microarray analysis. RNAs prepared using Qiagen RNeasy were from two separate pEhyg infections and two separate pEhyg-miR-146a infections. Each sample was labeled with Cy3 and with Cy5 to allow for dye swaps for each pair of pEhyg- and pEhyg-miR-146a-infected cells and hybridized to Agilent human 4 × 44,000 60-mer oligonucleotide arrays (Miltenyi Biotech). Data were processed and normalized using Rossetta Resolver software to identify genes from each infection pair showing greater-than-twofold differences and with P values of <0.01 (see Tables S1 and S2 in the supplemental material). To ensure that differences were reproducible in separate biological samples, differentially expressed genes in both infection sets were considered for further analysis.

Microarray data accession numbers. The raw array data have been published in the National Center for Biotechnology Information (NCBI) Gene Expression Omnibus (GEO) and assigned accession numbers GSM254072, GSM254076, GSM254077, GSM254081, GSM255655, GSM255656, GSM255658, GSM255659, and GSM255660. The series accession number for this work is GSE10107.

RESULTS

Cellular miRNAs are regulated by LMP1. EBV-negative derivatives of the Burkitt's lymphoma cell line, Mutu, were generated by transducing with a retrovirus expressing a dominant negative form of the EBV episomal replication/maintenance factor EBNA1. A resulting subclone confirmed to be EBV negative was transduced with either a control retroviral

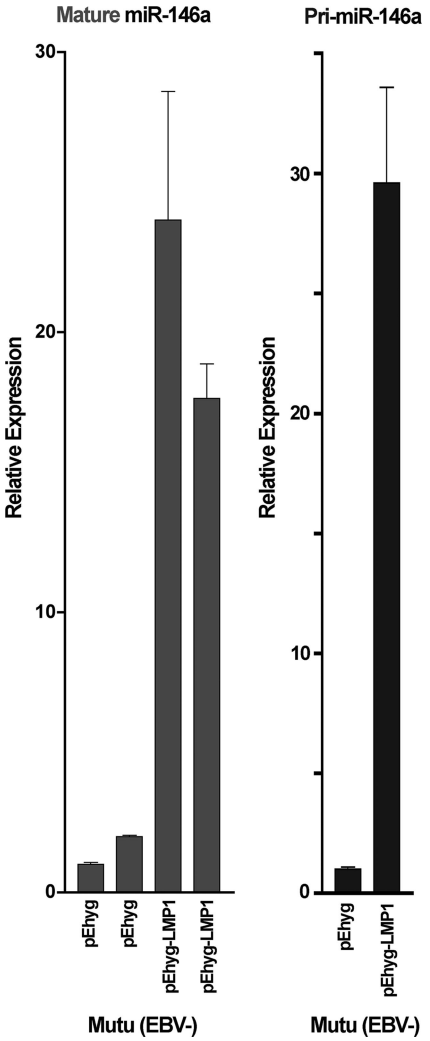

FIG. 2. qRT-PCR analysis of miR-146a expression. A. Mature miR-146a. Two separate preparations of RNA were isolated from EBV-negative Mutu-pEHyg and Mutu-pEHyg-LMP1 cells and analyzed by real-time PCR to assess levels of mature miR-146a. Data were normalized to U6 small nuclear RNA expression. B. Primary miR-146a. Total RNA isolated from EBV-negative Mutu-pEHyg and Mutu-pEHyg-LMP1 cells was reverse transcribed and used in a real-time PCR assay to detect the primary miR-146a transcript. Data were normalized to GAPDH expression.

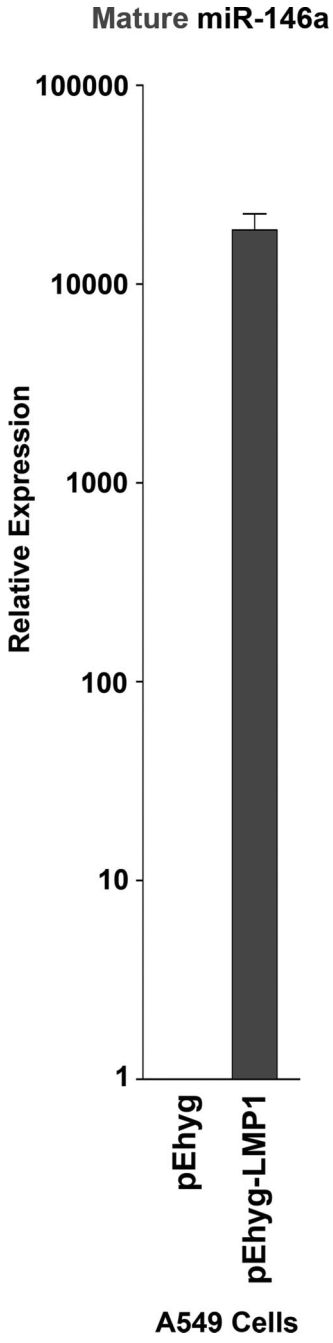

FIG. 3. LMP1 induces miR-146a in the epithelial cell line A549. Total RNA isolated from A549 lung epithelial cells transduced with pEHyg or pEHyg-FLAG-LMP1 retroviruses was polyadenylated, reverse transcribed, and used in a qPCR analysis of mature miR-146a expression. Data were normalized to U6 small nuclear RNA expression.

vector (pEhyg) or an LMP1-expressing retroviral vector (pEhyg-FLAG-LMP1). Cells were selected for 2 to 4 weeks in hygromycin prior to harvesting for total RNA preparations. Little cell death was observed during the selection procedure, indicating that retroviral transduction efficiency was high and that the resulting cell populations were highly polyclonal. Five separate RNA preparations were generated from control and LMP1-expressing cells, and the RNAs were size selected to isolate the small RNA fractions. Fractionated RNAs were then subjected to microRNA array analysis for expression of 470 unique human miRNAs. Data from five independent arrays were compiled (Fig. 1). Expression levels of 35 miRNAs were altered by LMP1 at $P < 0.05$, and of these, 15 miRNAs were regulated at the $P < 0.01$ level (10 induced by LMP1 and 5 suppressed by LMP1). In all five microarray assays, expression of miR-146a showed the highest level of differential expression (12- to 23-fold induction by LMP1), and we therefore focused on this miRNA for further analysis.

To confirm the results of the miRNA microarray analysis and to validate induction of the processed miR-146a transcript, qRT-PCR analysis was performed to assess the levels of ma-

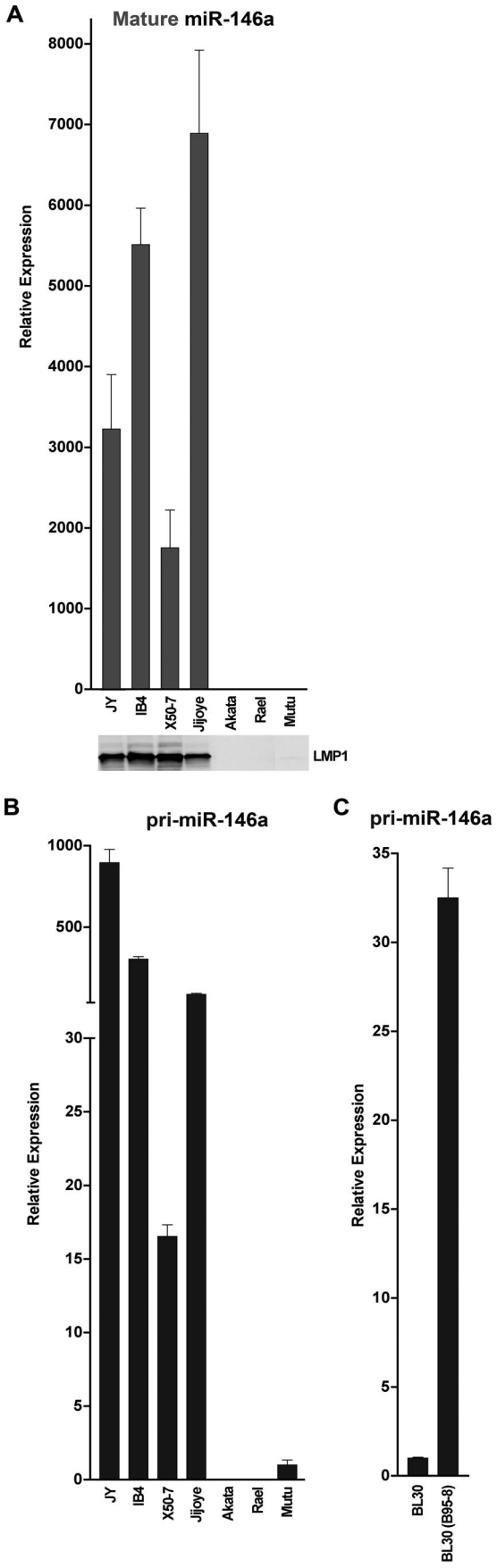

ture miR-146a in EBV-negative Mutu-pEHyg and Mutu-pEHyg-FLAG-LMP1 cells. As shown in Fig. 2A, quantitative RT-PCR analysis demonstrated induction of processed miR-146a. Since the related microRNAs miR-146a and miR-146b differ by only two nucleotides, analysis of the primary miR-146a transcript was carried out to more firmly establish LMP1-mediated regulation of the miR-146a locus. As shown in Fig. 2B, real-time RT-PCR analysis using pri-miR-146a-specific primers demonstrated elevated expression of pri-miR-146a in LMP1-expressing cells. Together, these results demonstrate that LMP1 induces the expression of pri-miR-146a and processed (mature) miR-146a.

LMP1 induces miR-146a expression in the epithelial cell line A549. In addition to its ability to transform B lymphocytes, EBV has also been linked to epithelial carcinoma of the nasopharynx (34). EBV-associated nasopharyngeal carcinomas display a type II latency expression pattern in which LMP1 is expressed (34). To determine if LMP1-mediated induction of miR-146a occurs in nonlymphoid cells, control and LMP1-expressing retroviruses were transduced into the lung epithelial cell line A549. Induction of mature miR-146a was detected in LMP1-transduced A549 cells compared to control transduced cells by qRT-PCR (Fig. 3), indicating that induction of miR-146a is not restricted to lymphoid tissues.

Mature miR-146a and pri-miR-146a are expressed in cells displaying type III but not type I latency gene expression patterns. To assess the level of miR-146a in an EBV-positive context where expression of LMP1 is naturally occurring, a panel of EBV-positive cell lines was examined by qRT-PCR. As shown in Fig. 4A, mature miR-146a was not detected in the type I Burkitt lymphoma cell lines Akata, Rael, and Mutu, which do not express LMP1. In contrast, high levels of miR-146a were detected in the type III cell lines JY, IB4, X50-7, and Jijoye, all of which express comparably high levels of LMP1. Analysis of the primary miR-146a transcript similarly showed significant differences between type III and type I latency cells, indicating that the differential expression levels in this cell panel are likely due in large part to differences in transcription (Fig. 4B).

The data in Fig. 4 provide evidence that EBV type III latency genes are responsible for the activated expression of miR-146a. To substantiate that the differential expression observed in type III versus type I cell lines is due to EBV gene expression and not clonal cell line differences, expression of

FIG. 4. Mature and primary miR-146a transcript analysis in a panel of cell lines. A. Total RNA isolated from EBV-positive, latency type III cell lines JY, IB4, X50-7 (lymphoblastoid cell lines), and Jijoye (Burkitt's lymphoma) and EBV-positive latency I Burkitt's lymphoma cell lines Akata, Rael, and Mutu was polyadenylated and reverse transcribed for qPCR analysis of mature miR-146a expression. The Western blot shows LMP1 expression in EBV latency type III cell lines but not in latency type I cell lines. B. Total RNA isolated from the indicated cell lines was reverse transcribed and subjected to qPCR to assess the levels of primary miR-146a transcripts. C. Total RNA extracted from the EBV-negative Burkitt's lymphoma cell line BL-30 and BL-30 cells infected with EBV B95-8 virus were reverse transcribed and assayed for pri-miR-146a expression by qPCR. Mature miR-146a expression was normalized to U6 small nuclear RNA expression, and pri-miR-146a expression was normalized to GAPDH expression.

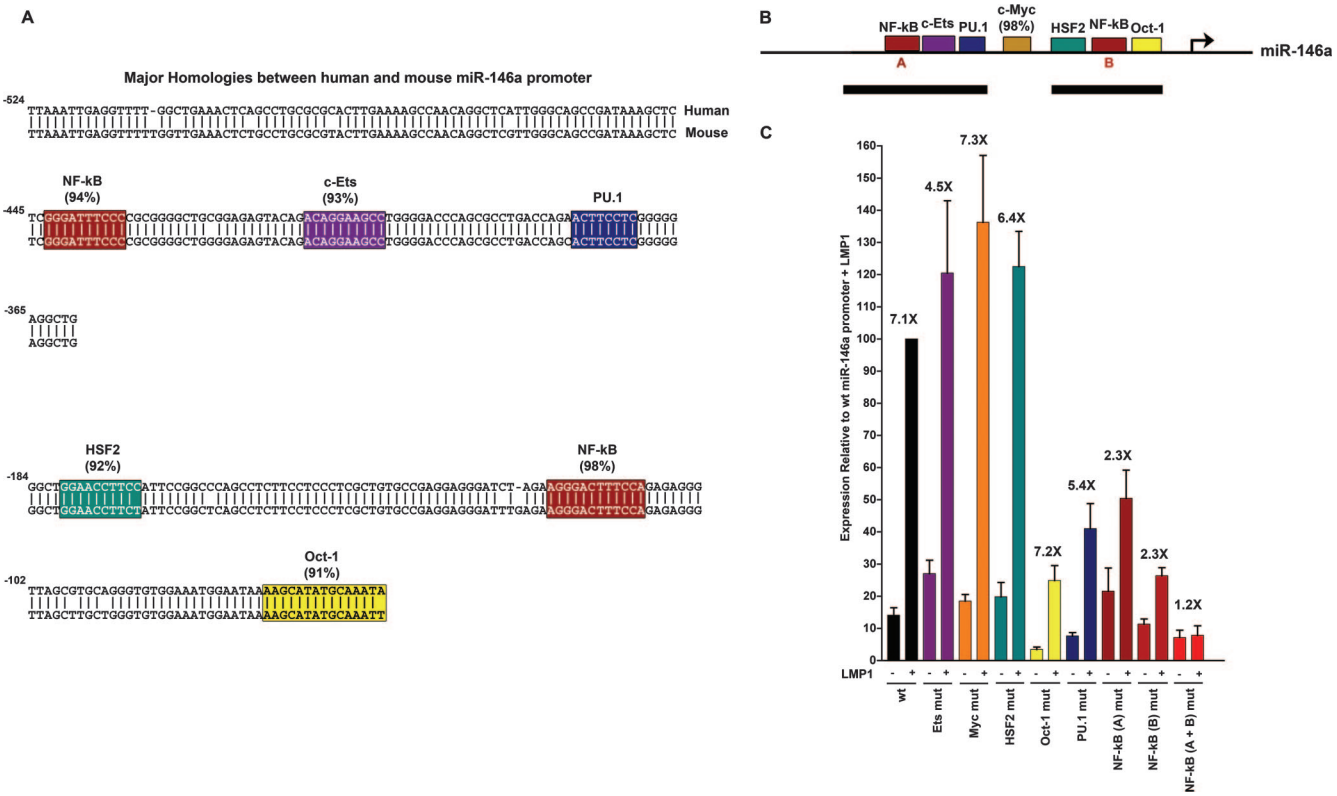

FIG. 5. miR-146a promoter analysis. A. Alignment of major homologies between human and mouse miR-146a promoter regions. Homologies were identified through a BLAST search using the human miR-146a promoter as described in Materials and Methods. Percentage scores for the indicated transcription factors were generated by TFSEARCH (http://www.cbrc.jp/research/db/TFSEARCH.html). B. Schematic representation of the human miR-146a promoter, with putative transcription factor binding sites. C. EBV-negative Mutu cells were cotransfected with pSG5 or pSG5-LMP1 plus wild-type or mutant miR-146a promoter-reporter vectors and harvested 48 h later. Luciferase expression is represented relative to luciferase activity of the wild-type promoter in the presence of LMP1. Error bars show the standard errors of the means. Increases for each reporter are indicated. Deletion of the dual NF-κB sites abrogated the ability of LMP1 to induce the miR-146a promoter.

pri-miR-146a transcripts were quantified in the EBV-negative Burkitt's lymphoma cell line BL30 and BL30 cells infected with the EBV strain B95-8 (which exhibit type III latency) (data not shown). As shown in Fig. 4C, EBV infection of BL30 cells induces expression of pri-miR-146a. Together, these results demonstrate that miR-146a is expressed in type III latency cells and that latency type III gene expression likely mediates induction of miR-146a.

LMP1 induces miR-146a expression through activation of two NF-κB elements in the miR-146a promoter. The experiments discussed above implicated a transcriptional mechanism for LMP1-mediated induction of miR-146a. To further address this issue, an approximately 1.2-kb region of the miR-146a promoter region was isolated from Mutu cells and cloned into a luciferase reporter plasmid. A BLAST search of the mouse genome using a 2-kb region of the human miR-146a promoter identified two significant homologies located in an analogous position relative to the miR-146a hairpin sequence. Visual inspection and analysis of these homologies using TFSEARCH (http://www.cbrc.jp/research/db/TFSEARCH.html) identified several high-probability transcription factor binding sites in the homologous regions, including two NF-κB sites previously identified by Taganov et al. (37) as well as potential c-Ets, PU.1, c-Myc, and Oct-1 sites. Each of these elements was mutated separately in the context of the miR-146a reporter plasmid. In addition, a mutant in which both NF-κB sites were disrupted was also generated. The wild-type or the mutant reporter plasmids were cotransfected into EBV-negative Mutu cells with either a control or an LMP1 expression vector. As shown in Fig. 5, expression of LMP1 enhanced the activity of the wild-type miR-146a reporter construct, as well as constructs containing mutations in the c-Myc, HSF2, and Oct-1 sites. Mutation of the PU.1 site marginally reduced the ability of LMP1 to induce expression from the miR-146a promoter ($P < 0.05$). Mutation of either NF-κB site substantially reduced the LMP1-mediated induction of the miR-146a promoter, and mutation of both NF-κB sites abrogated LMP1-mediated induction of miR-146a promoter expression ($P < 0.05$). These results indicate that LMP1 induces miR-146a expression primarily through activation of transcription via an NF-κB-dependent mechanism. Analysis of the Oct-1 site demonstrated that although mutation of this site does not alter the level of LMP1-mediated induction, the activity of this mutant is reduced in both control transfected as well as LMP1-transfected cells. This indicates that the Oct-1 site plays a substantive role in facilitating constitutive and induced expression of the miR-146a promoter and could therefore play a possible

TABLE 1. Transcripts induced in miR-146a-expressing Akata cells ($P < 0.01$)

Gene	Retrovirus infection (fold change)		Name and function
	Pair 1	Pair 2	
GIMAP4	7.4	7.7	GTPase, IMAP family member; decreased in T and B cells during activation
STON2[a]	2.9	2.7	Stonin 2; involved in endocytosis
AF086511	2.7	3.1	
AK022044	2.6	2.2	Protein tyrosine phosphatase,
(PTPRG)	2.1	2.0	receptor type, G; linked to
THC2247947	2.6	2.7	familial breast cancer; tumor suppressor
RAG1	2.5	2.5	Recombination activating gene 1; initiates V(D)J recombination during B-cell development
OSBPL1A	2.4	2.8	Oxysterol binding protein-like 1A; likely regulates lipid metabolism
SNTG2	2.3	3.0	Syntrophin; interacts with dystrophin

[a] Data were derived from array element AK094799.

role in mediating cell type-specific differences in miR-146a expression.

MicroRNA miR-146a suppresses interferon-responsive gene expression. To gain insights into the role that induction of miR-146a plays in influencing cellular responses, we generated an miR-146a retroviral expression vector and transduced it into Akata cells that do not express endogenous miR-146a. Duplicate infections of both the control retrovirus (pEhyg-miR-Control) and the miR-146a retrovirus (pEhyg-miR-146a) were carried out, and RNA was isolated from each infection 18 days later. The pEhyg-miR-146a-infected cells but not pEhyg-miR-Control-infected cells expressed the mature form of miR-146a (data not shown), indicating that the miR-146a transcript generated from this retrovirus undergoes appropriate microRNA processing. RNA preparations were then subjected to mRNA array analysis using a two-color Agilent 60-mer oligo $4 \times 44{,}000$ platform. Arrays were carried out on the duplicate infections, and dye swaps were analyzed for each. Genes showing greater-than-twofold differences in both sets of infections with P values of less than 0.01 were then compiled (see Tables S1 and S2 in the supplemental material for gene lists for each infection pair). As shown in Tables 1 to 3, eight genes were induced while 38 were suppressed by miR-146a. Of the 38 suppressed genes, 16 (42%) were identified as known interferon-inducible genes (Table 3). This suggests that miR-146a modulates a critical component(s) of the interferon signaling pathway. A higher proportion of genes that are not known to be interferon responsive contained potential 7-mer or better seed sequences (59%) than in the set of interferon-responsive genes (25%), indicating that regulation of most of the interferon-responsive genes likely occurs through a common upstream mediator (Tables 2 and 3; Fig. 6). The observed changes in

TABLE 2. Transcripts suppressed in miR-146a-expressing Akata cells (without known response to IFN) ($P < 0.01$)

Gene	Retrovirus infection (fold change)		miR-146a seed match	Name and/or function
	Pair 1	Pair 2		
DNAPTP6	−7.2	−12.0	8-mer	DNA polymerase-transactivated protein 6; transactivated by viral polymerase
SAMD9L	−7.5	−5.8	Two 7-mers	Sterile α-motif domain-containing 9-like
EPSTI1[a]	−6.5	−6.0	9-mer	Epithelial stromal interaction 1; induced in tumor cells cocultivated with fibroblasts
EPSTI1	−4.0	−4.8		
RGS13	−5.3	−6.8	None	Regulator of G-protein signaling 13; may mediate cytokine signaling in germinal centers; suppressed by EBV LMP1
HSPA1A	−4.2	−2.0	10-mer	Heat shock 70-kDa protein 1A, HSP72; antiapoptotic
BCL2A1	−4.0	−3.0	7-mer	Bcl2-related protein A1; induced by NF-κB, EBV-LMP1, and EBNA2; antiapoptotic
BG547557	−4.0	−3.5		
CCR9	−3.5	−4.0	11-mer	Chemokine (c-c motif) receptor 9; receptor for TECK, involved in mucosal homing of lymphocytes
PPP1R1C	−3.5	−2.7	None	
AK026784	−3.5	−2.8	7-mer	
FLJ10986	−3.4	−3.5	8-mer	
FLJ10986	−2.7	−3.2		
ITGBL1[a]	−3.1	−4.5	None	Integrin β-like 1
C1ORF21 (PIG13)	−3.1	−2.1	7-mer	Proliferation-induced gene 13
C1ORF21 (PIG13)	−2.7	−2.1		
OLFML2A	−2.9	−2.2	7-mer	Olfactomedin-like 2A
KIAA0774	−2.7	−2.2	12-mer	
KIAA0774	−2.7	−3.7		
C16ORF81[a]	−2.6	−2.7	None	
ZBTB32	−2.6	−2.6	None	Zinc finger and BTB domain-containing 32; transcription factor involved in osteoblastic differentiation
AK057704	−2.4	−2.0	None	
TMTC2	−2.3	−2.2	None	Transmembrane and tetracopeptide repeat-containing 2
SYT12	−2.1	−2.0	9-mer, two 7-mers	Synaptotagmin XII, or SRG1; involved in brain disorders
ITGB2	−2.0	−2.0	7-mer	Integrin, β2
LMO2	−2.0	−2.0	None	LIM domain only 2 (rhombotin-like 1)

[a] Data were derived from the following array elements: EPSTI1 (ENST00000313624), ITGBL1 (ENST00000376155), and C16ORF81 (ENST00000270031).

TABLE 3. Transcripts suppressed in miR-146a-expressing Akata cells (known to be IFN responders) ($P < 0.01$)

Gene	Retrovirus infection (fold change)		miR-146a seed match	Name and/or function
	Pair 1	Pair 2		
IFI44L	−9.2	−9.7	None	Interferon-induced protein 44-like, or histocompatibility 28
IFI44	−7.4	−7.8	None	Interferon-induced protein 44; induced during hepatitis virus infection
MX2	−4.6	−4.9	7-mer	Myxovirus (influenza virus) resistance 2, or interferon-induced GTP binding protein MXB
MX2	−3.9	−3.5		
RSAD2	−4.4	−3.0	None	Radical *S*-adenosyl methionine domain-containing 2, or viperin; antiviral; induced during TLR signaling
RSAD2	−2.5	−2.7		
IFIT3	−3.9	−3.0	Two 8-mers	Interferon-induced protein with tetratricopeptide repeats 3
OASL	−3.2	−2.6	7-mer	2′-5′-oligoadenylate synthetase-like; binds double-stranded RNA and DNA
TRIM22	−2.9	−2.7	Two 7-mers	Tripartite motif-containing 22, or STAF50; can inhibit viral replication
TRIM22	−2.7	−2.7		
IFIT1	−3.3	−3.2	None	Interferon-induced protein with tetratricopeptide repeats 1
IFIT5	−2.7	−2.8	None	Interferon-induced protein with tetratricopeptide repeats 5
IFIT5	−2.8	−2.5		
IFITM1	−2.4	−2.7	None	Interferon-induced transmembrane protein 1, LEU13, or CD225; regulates cell growth
IFITM3	−2.7	−2.3	None	Interferon-induced transmembrane protein 3
IFITM3[a]	−2.4	−2.4		
IFITM3[a]	−2.4	−2.5		
IFITM4P	−2.7	−2.9	None	Interferon-induced transmembrane protein 4 pseudogene
IRF7	−2.3	−2.5	None	Interferon regulatory factor 7; transcriptional activator in response to infection; binds to Qp of EBV EBNA1; involved in TLR signaling; colocalizes with and regulates EBV LMP1
IRF7	−2.6	−2.5		
NMI	−2.7	−2.9	None	N-myc (and STAT) interactor; transcription factor induced by interferon
ISG15	−2.1	−2.1	None	ISG15 ubiquitin-like modifier; targets STAT1, MAPK3, JAK1, etc; antiviral properties
IFI27	−2.3	−2.3	None	Alpha interferon-inducible protein 27
IFI27	−2.4	−2.6		

[a] Data were derived from the array element ENST00000313624.

mRNA expression in miR-146a-expressing Akata cells are not likely due to artifacts generated by expressing RNA of a double-stranded nature, since there was little similarity in altered gene expression patterns in Akata cells transduced with other miRNA-expressing retroviruses (miR-155 and miR-21) compared to miR-146a-transduced Akata cells (unpublished).

DISCUSSION

MicroRNAs have been shown to play important regulatory roles in a wide variety of cellular processes, including cell cycle progression, differentiation, apoptosis, and signaling. In addition, a number of groups have reported the altered expression of miRNAs in various forms of human cancers. Viruses regularly exploit cellular pathways in order to complete the viral life cycle. Although EBV and other herpesviruses encode their own set of microRNAs, the extent to which DNA tumor viruses utilize cellular miRNA pathways during infection has not been explored. We have shown here that LMP1, the major oncoprotein of the human tumor virus EBV, alters the expression profile of several cellular miRNA species, including the most highly regulated of these, miR-146a. Induction of miR-146a likely occurs during the natural course of EBV infection, since miR-146a is highly expressed in EBV-positive cells exhibiting type III latency gene expression (but not type I latency) and infection of EBV-negative cells with EBV induces the expression of miR-146a.

While regulation of microRNA expression can occur at a number of different processing levels, it is clear that LMP1 induces the transcription of miR-146a, since LMP1 increases primary miR-146a transcript levels and activates a reporter plasmid containing the miR-146a promoter. As expected, induction of the miR-146a promoter occurs to a large extent through two conserved NF-κB transcription factor binding sites. These data are in line with a recent report demonstrating NF-κB-dependent induction of miR-146a expression by TLR signaling (by TLR-2, -4, and -5 [37]), emphasizing the importance of the NF-κB sites in mediating the activation of miR-146a expression by various signaling molecules. In contrast, however, although Taganov et al. also demonstrated induction of two other microRNAs by TLR signaling, miR-155 and miR-132 (37), our array analysis did not reveal the induction of either of these, and we have not been able to demonstrate substantial induction of miR-155 by LMP1 in a number of systems despite the presence of candidate NF-κB and AP-1 promoter elements in the miR-155 promoter (Q. Yin and E. Flemington, unpublished data). Although the differential responses of miR-155 and miR-132 to TLR and LMP1 signaling may reflect biological differences between monocytes (Taganov et al. [37]) and B lymphocytes (this study), it may on the other hand suggest that TLR and LMP1 elicit similar but distinct signaling pathways which result in differential miRNA induction profiles.

In addition to NF-κB, LMP1 induces a number of other transcription factor pathways (p38/mitogen-activated protein kinase/activator transcription factor 2, cJUN/c-Jun N-terminal kinase/AP-1, and phosphatidylinositol 3-kinase/Akt) (reviewed in reference 23) and is known to induce some genes through

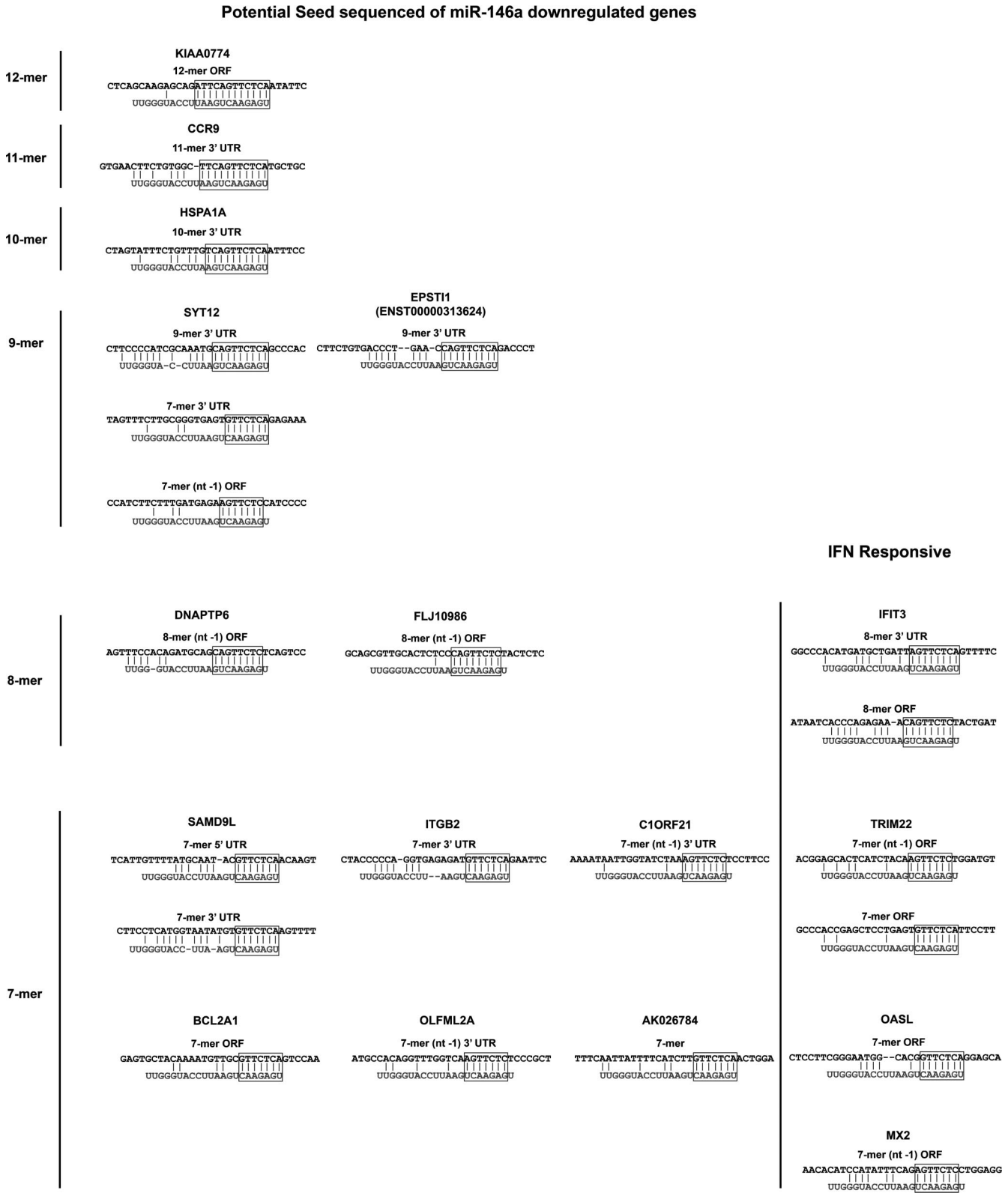

FIG. 6. Down-regulated genes with 7-mer or better miR-146a seed sequences. Transcript sequences were obtained from the website www.ensembl.org.

c-Ets sites (21). Nevertheless, despite the presence of a potential c-Ets site within the conserved region of the miR-146a promoter, we did not see an evident role for this element in activation of the miR-146a reporter. Additional experiments using a natural genomic context and/or other cell systems are required to address this issue more thoroughly.

It is notable that the expression of miR-146a in latency type III cells is significantly higher than that of EBV-negative cells infected with an LMP1 retrovirus. It is unclear what may account for this difference. It is possible that the genetic background of Mutu cells is less favorable for LMP1 signaling than the type III latency cell types assessed in our studies. Another plausible explanation is possible cooperative induction of miR-146a by LMP1 and other type III latency genes. For example, EBNA-3C has been shown to activate gene expression through PU.1 promoter elements (43), and the conserved PU.1 site in the miR-146a promoter could be influenced by EBNA-3C. Notably, mutation of this element had a moderate but significant inhibitory effect on the miR-146a promoter, suggesting that this element contributes to promoter function.

The miR-146a promoter also contains a highly conserved Octamer binding site (Oct-1) near the TATA box that contributes substantially to both basal and induced miR-146a promoter activity. While a number of Octamer binding proteins have been identified that bind to prototypical Oct-1 elements, this element was shown early on to confer B-cell-specific expression of the immunoglobulin genes (28). This element may therefore play a role in conferring at least some level of lymphocyte specificity for miR-146a and may contribute to induction of miR-146a by various lymphocyte-stimulating agents. Nevertheless, it is clear that miR-146a can be expressed in other tissues (such as A549 cells infected with an LMP1 retrovirus), and the Oct-1 site may or may not be required for this activity. It is notable that the closely related miRNA, miR-146b, was only marginally induced by LMP1 (less than twofold induction; $P < 0.05$). MicroRNAs miR-146a and miR-146b have identical 5′ ends, which are the regions of microRNAs that appear to play the predominant role in specific binding and inhibition of mRNAs (30). Although these two miRNAs share many of the same targets, it appears that the regulation of miR-146b is distinct at least in some ways from that of miR-146a. Such distinct regulatory mechanisms for cognate microRNAs may be a way to elicit the same downstream response in different tissues or under different conditions.

Cellular miRNA expression alters the expression level of some (but not all) mRNA transcripts directly targeted by miRNAs. In addition, miRNA modulation of protein expression also impacts the expression of mRNA transcripts downstream of the modulated proteins within the biological pathway. Therefore, we employed mRNA transcriptional microarray profiling to simultaneously shed light on the direct targets of miR-146a and the cellular pathway(s) impacted by miR-146a expression. Our array analysis of miR-146a-expressing Akata cells revealed a group of miR-146a-suppressed genes that are known to be responsive to interferon signaling. This indicates that miR-146a may be part of a negative feedback loop that plays a role in modulating the interferon response. This could be a means of fine-tuning the level of interferon signaling and/or could be a means of providing a shut-off mechanism following stimulation during normal physiological signaling. Interestingly, like miR-155, elevated miR-146a has been correlated with certain tumor types (13, 39, 41). It is possible that the inappropriate expression of miR-146a could lead to suppression of the interferon response pathway in tumors, thereby helping suppress immune-mediated surveillance through interferon signaling. In the context of EBV infection, induction of miR-146a could result in suppression or modulation of the interferon-mediated antiviral response, protecting the virus from host immunity. It is interesting that the interferon pathway itself has been shown to induce cellular miRNAs that inhibit hepatitis C virus replication, indicating that cellular miRNA induction during viral infection can be either productive or deleterious to the virus (33).

One of the interferon-related genes found here to be suppressed by miR-146a is the transcriptional activator IRF7, which has been shown to bind and activate the LMP1 promoter (31). It is therefore likely that a more direct consequence of miR-146a expression on interferon signaling is the negative feedback regulation of LMP1 expression itself. This may be a means of establishing a refined regulation of LMP1 expression to avoid some of the known deleterious effects of overexpressed LMP1.

Our initial target analysis of miR-146a-regulated genes discussed above did not reveal any potential direct miR-146a targets that may play a role in mediating disruption of the interferon signaling pathway. Although the ability of microRNAs to inhibit translation of target mRNAs is clear, the contribution of microRNA-mediated degradation of target mRNAs is much less well understood, and it is thought that only a subset of mRNAs may be subject to degradation. Therefore, a key target of miR-146a involved in the interferon signaling pathway may not be revealed by analyzing RNA levels and may only be detected by assessing protein expression. Taganov et al. previously demonstrated that reporter plasmids containing the 3′ UTRs of TRAF6 and IRAK1 were suppressed by miR-146a (37), but they did not assess whether endogenous TRAF6 or IRAK1 (RNA or protein) levels were influenced by miR-146a. Our array analysis showed no alteration of TRAF6 RNA levels in either miR-146a infection pair; however, expression of IRAK1 was suppressed in the first infection set by more than the twofold cutoff, while it was suppressed in the second infection set by just less than the twofold cutoff (-1.9) (Fig. 7; see also Tables S1 and S2 in the supplemental material). It is therefore possible that suppression of IRAK1 expression could play a role in mediating the miR-146a feedback mechanism. It is of note that IRF7 resides downstream of both TRAF6 and IRAK1 in antiviral TLR7/8 signaling (38). Since no direct miR-146a target site was identified in the IRF7 transcript, it is possible that the regulation of IRF7 occurs through miR-146a-mediated regulation of IRAK1 and/or TRAF6. The regulation of IRF7 would in turn limit production of IFN-α (14), thereby limiting the antiviral response. We also noted that a more direct mediator of interferon signaling, signal transducer and activator of transcription 1 (STAT1), was similarly missed in our analysis, since it was suppressed above our threshold in only one experiment while it was suppressed by 1.8- to 1.9-fold in the second experiment (Fig. 7; see also Tables S1 and S2 in the supplemental material). In addition, we identified an 8-mer miR-146a seed sequence in the 3′ UTR of STAT1 (ensembl.org transcript) (Fig.

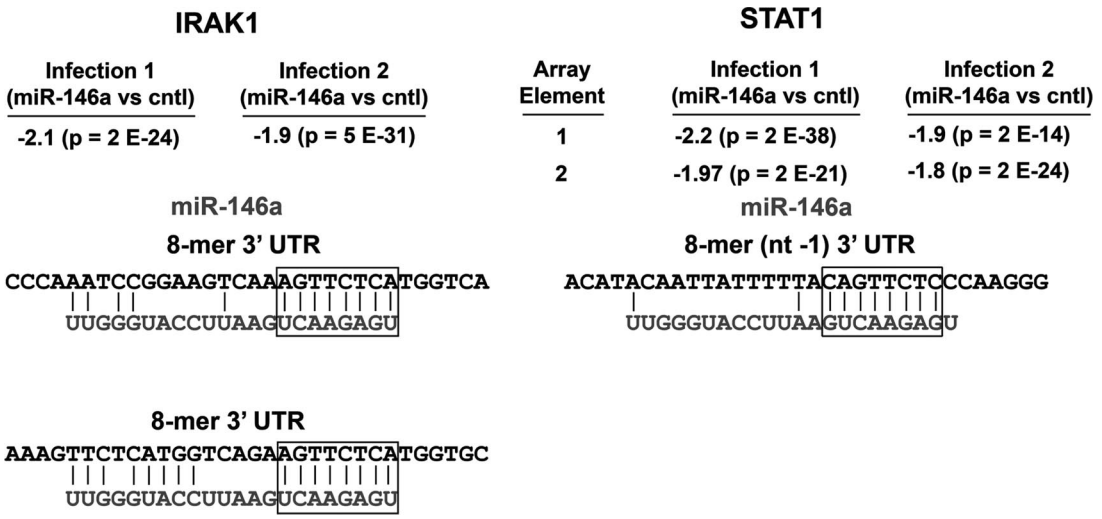

FIG. 7. Differential expression levels of IRAK1 and STAT1 in miR-146a versus control cells. Potential seed sequences are shown. Transcript sequences were obtained from the website www.ensembl.org.

7). While IRAK1 and STAT1 are possible candidates for direct mediators of interferon suppression, STAT1 is interesting since it is more directly upstream of activation of interferon-responsive genes.

Despite the possible negative feedback mechanism, it is likely that miR-146a also targets other pathways. In this context, we note that although LMP1 induces the expression of a relatively large number of genes, it has also been shown to suppress the expression of some genes, one of which is RGS13 (4). As shown in Table 2, miR-146a suppresses the expression of RGS13, suggesting that LMP1 may suppress RGS13 (and perhaps other genes) in part through the induction of miR-146a.

ACKNOWLEDGMENTS

Support for this project was provided by funding from the Tulane Cancer Center and grants awarded to E. Flemington by the National Institutes of Health (R01-GM48045, R21-DE17008, and R01 CA124311). Support was also provided by a National Institutes of Health COBRE grant, P20 RR020152.

We thank Nancy Raab-Traub for providing the CMV-FLAG-LMP1 vector. We also thank Xiaochuan Zhou and LC Sciences for miRNA microarray expertise and Xiaofeng Hu (Tulane Cancer Genetic Core) for her expertise with the Agilent microarray studies.

REFERENCES

1. **Akira, S., and K. Takeda.** 2004. Toll-like receptor signalling. Nat. Rev. Immunol. **4:**499–511.
2. **Bolstad, B. M., R. A. Irizarry, M. Astrand, and T. P. Speed.** 2003. A comparison of normalization methods for high density oligonucleotide array data based on variance and bias. Bioinformatics **19:**185–193.
3. **Brodeur, S. R., G. Cheng, D. Baltimore, and D. A. Thorley-Lawson.** 1997. Localization of the major NF-κB-activating site and the sole TRAF3 binding site of LMP-1 defines two distinct signaling motifs. J. Biol. Chem. **272:**19777–19784.
4. **Cahir-McFarland, E. D., K. Carter, A. Rosenwald, J. M. Giltnane, S. E. Henrickson, L. M. Staudt, and E. Kieff.** 2004. Role of NF-κB in cell survival and transcription of latent membrane protein 1-expressing or Epstein-Barr virus latency III-infected cells. J. Virol. **78:**4108–4119.
5. **Costinean, S., N. Zanesi, Y. Pekarsky, E. Tili, S. Volinia, N. Heerema, and C. M. Croce.** 2006. Pre-B cell proliferation and lymphoblastic leukemia/high-grade lymphoma in E(mu)-miR155 transgenic mice. Proc. Natl. Acad. Sci. USA **103:**7024–7029.
6. **Devergne, O., E. Hatzivassiliou, K. M. Izumi, K. M. Kaye, M. F. Kleijnen, E. Kieff, and G. Mosialos.** 1996. Association of TRAF1, TRAF2, and TRAF3 with an Epstein-Barr virus LMP1 domain important for B-lymphocyte transformation: role in NF-κB activation. Mol. Cell. Biol. **16:**7098–108.
7. **Eisen, M. B., P. T. Spellman, P. O. Brown, and D. Botstein.** 1998. Cluster analysis and display of genome-wide expression patterns. Proc. Natl. Acad. Sci. USA **95:**14863–14868.
8. **Eliopoulos, A. G., S. M. Blake, J. E. Floettmann, M. Rowe, and L. S. Young.** 1999. Epstein-Barr virus-encoded latent membrane protein 1 activates the JNK pathway through its extreme C terminus via a mechanism involving TRADD and TRAF2. J. Virol. **73:**1023–1035.
9. **Eliopoulos, A. G., N. J. Gallagher, S. M. Blake, C. W. Dawson, and L. S. Young.** 1999. Activation of the p38 mitogen-activated protein kinase pathway by Epstein-Barr virus-encoded latent membrane protein 1 coregulates interleukin-6 and interleukin-8 production. J. Biol. Chem. **274:**16085–16096.
10. **Eliopoulos, A. G., and L. S. Young.** 1998. Activation of the cJun N-terminal kinase (JNK) pathway by the Epstein-Barr virus-encoded latent membrane protein 1 (LMP1). Oncogene **16:**1731–1742.
11. **Gires, O., U. Zimber-Strobl, R. Gonnella, M. Ueffing, G. Marschall, R. Zeidler, D. Pich, and W. Hammerschmidt.** 1997. Latent membrane protein 1 of Epstein-Barr virus mimics a constitutively active receptor molecule. EMBO J. **16:**6131–6140.
12. **Hatzivassiliou, E., W. E. Miller, N. Raab-Traub, E. Kieff, and G. Mosialos.** 1998. A fusion of the EBV latent membrane protein-1 (LMP1) transmembrane domains to the CD40 cytoplasmic domain is similar to LMP1 in constitutive activation of epidermal growth factor receptor expression, nuclear factor-kappa B, and stress-activated protein kinase. J. Immunol. **160:**1116–1121.
13. **He, H., K. Jazdzewski, W. Li, S. Liyanarachchi, R. Nagy, S. Volinia, G. A. Calin, C. G. Liu, K. Franssila, S. Suster, R. T. Kloos, C. M. Croce, and A. de la Chapelle.** 2005. The role of microRNA genes in papillary thyroid carcinoma. Proc. Natl. Acad. Sci. USA **102:**19075–19080.
14. **Honda, K., H. Yanai, H. Negishi, M. Asagiri, M. Sato, T. Mizutani, N. Shimada, Y. Ohba, A. Takaoka, N. Yoshida, and T. Taniguchi.** 2005. IRF-7 is the master regulator of type-I interferon-dependent immune responses. Nature **434:**772–777.
15. **Huye, L. E., S. Ning, M. Kelliher, and J. S. Pagano.** 2007. Interferon regulatory factor 7 is activated by a viral oncoprotein through RIP-dependent ubiquitination. Mol. Cell. Biol. **27:**2910–2918.
16. **Izumi, K. M., E. D. Cahir McFarland, A. T. Ting, E. A. Riley, B. Seed, and E. D. Kieff.** 1999. The Epstein-Barr virus oncoprotein latent membrane protein 1 engages the tumor necrosis factor receptor-associated proteins TRADD and receptor-interacting protein (RIP) but does not induce apoptosis or require RIP for NF-κB activation. Mol. Cell. Biol. **19:**5759–5767.
17. **Izumi, K. M., K. M. Kaye, and E. D. Kieff.** 1997. The Epstein-Barr virus LMP1 amino acid sequence that engages tumor necrosis factor receptor associated factors is critical for primary B lymphocyte growth transformation. Proc. Natl. Acad. Sci. USA **94:**1447–1452.
18. **Izumi, K. M., and E. D. Kieff.** 1997. The Epstein-Barr virus oncogene product latent membrane protein 1 engages the tumor necrosis factor receptor-associated death domain protein to mediate B lymphocyte growth transformation and activate NF-κB. Proc. Natl. Acad. Sci. USA **94:**12592–12597.
19. **Kaye, K. M., K. M. Izumi, G. Mosialos, and E. Kieff.** 1995. The Epstein-Barr virus LMP1 cytoplasmic carboxy terminus is essential for B-lymphocyte

transformation; fibroblast cocultivation complements a critical function within the terminal 155 residues. J. Virol. **69:**675–683.
20. **Kieff, E. D., and A. B. Rickinson.** 2007. Epstein-Barr virus and its replication, p. 2603–2654. *In* D. M. Knipe, P. M. Howley, D. E. Griffin, R. A. Lamb, M. A. Martin, B. Roizman, and S. E. Straus (ed.), Fields virology, 5th ed., vol. 2. Lippincott Williams & Wilkins, Philadelphia, PA.
21. **Kondo, S., N. Wakisaka, M. J. Schell, T. Horikawa, T. S. Sheen, H. Sato, M. Furukawa, J. S. Pagano, and T. Yoshizaki.** 2005. Epstein-Barr virus latent membrane protein 1 induces the matrix metalloproteinase-1 promoter via an Ets binding site formed by a single nucleotide polymorphism: enhanced susceptibility to nasopharyngeal carcinoma. Int. J. Cancer **115:**368–376.
22. **Kulwichit, W., R. H. Edwards, E. M. Davenport, J. F. Baskar, V. Godfrey, and N. Raab-Traub.** 1998. Expression of the Epstein-Barr virus latent membrane protein 1 induces B cell lymphoma in transgenic mice. Proc. Natl. Acad. Sci. USA **95:**11963–11968.
23. **Li, H. P., and Y. S. Chang.** 2003. Epstein-Barr virus latent membrane protein 1: structure and functions. J. Biomed. Sci. **10:**490–504.
24. **Liebowitz, D., D. Wang, and E. Kieff.** 1986. Orientation and patching of the latent infection membrane protein encoded by Epstein-Barr virus. J. Virol. **58:**233–237.
25. **Liu, J., F. V. Rivas, J. Wohlschlegel, J. R. Yates III, R. Parker, and G. J. Hannon.** 2005. A role for the P-body component GW182 in microRNA function. Nat. Cell Biol. **7:**1261–1266.
26. **Liu, J., M. A. Valencia-Sanchez, G. J. Hannon, and R. Parker.** 2005. MicroRNA-dependent localization of targeted mRNAs to mammalian P-bodies. Nat. Cell Biol. **7:**719–723.
27. **Lytle, J. R., T. A. Yario, and J. A. Steitz.** 2007. Target mRNAs are repressed as efficiently by microRNA-binding sites in the 5′ UTR as in the 3′ UTR. Proc. Natl. Acad. Sci. USA **104:**9667–9672.
28. **Matthias, P.** 1998. Lymphoid-specific transcription mediated by the conserved octamer site: who is doing what? Semin. Immunol. **10:**155–163.
29. **Mosialos, G., M. Birkenbach, R. Yalamanchili, T. VanArsdale, C. Ware, and E. Kieff.** 1995. The Epstein-Barr virus transforming protein LMP1 engages signaling proteins for the tumor necrosis factor receptor family. Cell **80:**389–399.
30. **Nielsen, C. B., N. Shomron, R. Sandberg, E. Hornstein, J. Kitzman, and C. B. Burge.** 2007. Determinants of targeting by endogenous and exogenous microRNAs and siRNAs. RNA **13:**1894–1910.
31. **Ning, S., A. M. Hahn, L. E. Huye, and J. S. Pagano.** 2003. Interferon regulatory factor 7 regulates expression of Epstein-Barr virus latent membrane protein 1: a regulatory circuit. J. Virol. **77:**9359–9368.
32. **Pan, W.** 2002. A comparative review of statistical methods for discovering differentially expressed genes in replicated microarray experiments. Bioinformatics **18:**546–554.
33. **Pedersen, I. M., G. Cheng, S. Wieland, S. Volinia, C. M. Croce, F. V. Chisari, and M. David.** 2007. Interferon modulation of cellular microRNAs as an antiviral mechanism. Nature **449:**919–922.
34. **Rickinson, A. B., and E. Kieff.** 2007. Epstein-Barr virus, p. 2655–2700. *In* D. M. Knipe, P. M. Howley, D. E. Griffin, R. A. Lamb, M. A. Martin, B. Roizman, and S. E. Straus (ed.), Fields virology, 5th ed., vol. 2. Lippincott Williams & Wilkins, Philadelphia, PA.
35. **Rodriguez, A., E. Vigorito, S. Clare, M. V. Warren, P. Couttet, D. R. Soond, S. van Dongen, R. J. Grocock, P. P. Das, E. A. Miska, D. Vetrie, K. Okkenhaug, A. J. Enright, G. Dougan, M. Turner, and A. Bradley.** 2007. Requirement of bic/microRNA-155 for normal immune function. Science **316:**608–611.
36. **Schaefer, B. C., T. C. Mitchell, J. W. Kappler, and P. Marrack.** 2001. A novel family of retroviral vectors for the rapid production of complex stable cell lines. Anal. Biochem. **297:**86–93.
37. **Taganov, K. D., M. P. Boldin, K. J. Chang, and D. Baltimore.** 2006. NF-κB-dependent induction of microRNA miR-146, an inhibitor targeted to signaling proteins of innate immune responses. Proc. Natl. Acad. Sci. USA **103:**12481–12486.
38. **Uematsu, S., S. Sato, M. Yamamoto, T. Hirotani, H. Kato, F. Takeshita, M. Matsuda, C. Coban, K. J. Ishii, T. Kawai, O. Takeuchi, and S. Akira.** 2005. Interleukin-1 receptor-associated kinase-1 plays an essential role for Toll-like receptor (TLR)7- and TLR9-mediated interferon-α induction. J. Exp. Med. **201:**915–923.
39. **Volinia, S., G. A. Calin, C. G. Liu, S. Ambs, A. Cimmino, F. Petrocca, R. Visone, M. Iorio, C. Roldo, M. Ferracin, R. L. Prueitt, N. Yanaihara, G. Lanza, A. Scarpa, A. Vecchione, M. Negrini, C. C. Harris, and C. M. Croce.** 2006. A microRNA expression signature of human solid tumors defines cancer gene targets. Proc. Natl. Acad. Sci. USA **103:**2257–2261.
40. **West, A. B., G. Kapatos, C. O'Farrell, F. Gonzalez-de-Chavez, K. Chiu, M. J. Farrer, and N. T. Maidment.** 2004. N-myc regulates Parkin expression. J. Biol. Chem. **279:**28896–28902.
41. **Yanaihara, N., N. Caplen, E. Bowman, M. Seike, K. Kumamoto, M. Yi, R. M. Stephens, A. Okamoto, J. Yokota, T. Tanaka, G. A. Calin, C. G. Liu, C. M. Croce, and C. C. Harris.** 2006. Unique microRNA molecular profiles in lung cancer diagnosis and prognosis. Cancer Cell **9:**189–198.
42. **Young, L. S., and P. G. Murray.** 2003. Epstein-Barr virus and oncogenesis: from latent genes to tumours. Oncogene **22:**5108–5121.
43. **Zhao, B., and C. E. Sample.** 2000. Epstein-Barr virus nuclear antigen 3C activates the latent membrane protein 1 promoter in the presence of Epstein-Barr virus nuclear antigen 2 through sequences encompassing an spi-1/Spi-B binding site. J. Virol. **74:**5151–5160.